Comparisons of the Soot Volume Fraction Using Gravimetric and Light Extinction Techniques

M. Y. CHOI
Department of Mechanical Engineering, University of Illinois at Chicago, Chicago, IL 60607

G. W. MULHOLLAND, A. HAMINS and T. KASHIWAGI
Building and Fire Research Laboratory, NIST, Gaithersburg, MD 20899

Simultaneous optical and gravimetric measurements were performed in the postflame region of an acetylene/air premixed flame where the temperature of the soot/gas mixture was reduced to 500 K through nitrogen dilution. By combining gravimetric measurements of the collected soot with soot density measurements using helium pycnometry, an accurate value of the soot volume fraction was obtained. The temperature and soot concentration profiles were measured to compare the line of sight light extinction measurement with the point sampling gravimetric measurements. The soot volume fraction obtained by light extinction measurements overestimated the actual soot volume fraction by about a factor of two. By calibrating the optical measurements with the gravimetric soot volume fractions, a dimensionless extinction coefficient, K_e, of 8.6 was measured. This value is conjectured to be applicable for soot generated for a variety of fuels and to be valid for extinction wavelengths in the visible to the near-infrared. It was also found that the mass specific light extinction coefficient was found to be 8.0 m^2/g which is consistent with measurements reported in the literature for a variety of fuels.

INTRODUCTION

Determination of the soot volume fraction using laser extinction measurements is a technique that is widely used in the combustion community. It is an attractive technique because it provides an instantaneous, nonintrusive measurement. This technique is used both within the combustion zone and in the postflame region. Within the flame, the soot volume fraction measurement is central to the study of soot growth [1, 2] and for studying the radiant transport [3, 4]. It has been found that thermal radiation from soot dominates the heat feedback to the fuel surface for large fires [5, 6]. In the postflame region, the light extinction measurements are used in estimating not only the soot volume fraction but also the soot yield and the specific extinction coefficient per mass of fuel consumed [7, 8]. Such information is important in the detection of fires, in assessing the reduction in visibility arising from a fire in a building [9] and for estimating the health and environmental impact of large fires [10].

Even though the soot volume fraction is a key property for describing soot both in the flame and above the flame, there has been little work to verify the accuracy of measurements by light extinction techniques. Choi et al. [11] studied the effects of source wavelength, scattering by soot particles, light extinction by "large" molecules and the use of different indices of refraction reported in the literature on the measurement of soot volume fraction. The experiments indicated that the measured soot volume fractions were sensitive to the absorption constant (which was calculated using the reported refractive indices). For example, at a wavelength of 632.8 nm, the absorption constant can vary by a factor of two depending on the choice of indices of refraction [11].

The focus of this paper is on the development of an independent method for characterizing soot volume fraction to assess the accuracy and to calibrate the light extinction method. In short, the method consists of isokinetically sampling the soot at a known flow rate, measuring the mass of soot collected, and determining the density of the soot by helium pycnometry. The optical measurements can then be calibrated with the gravimetric measurements. In this manner, the dimensionless extinction constant can be determined without making assumptions regarding the optical properties of soot which can introduce significant uncertainties. The accurate measurement of the dimensionless extinction constant can

COMBUSTION AND FLAME 102: 161–169 (1995)

Published by Elsevier Science Inc.

0010-2180/95/$9.50
SSDI 0010-2180(94)00282-W

Nos. 1/2

"light" tubes with a small N_2 purge flow (see Location B in Fig. 1). The 2.1-cm-diameter tripper plate increased mixing and reduced the fluctuations in the transmitted intensity compared to a 6.5-cm-diameter tripper plate. Although this improved the uniformity of smoke over the chimney cross section and reduced the fluctuations, it was important to characterize the temperature and smoke concentration profiles to make a quantitative comparison between the optical and gravimetric soot volume fraction measures.

Inevitably, there were deposits of soot on the inner surface of the stainless-steel probe. Soot that was used to calculate the gravimetrically-measured soot volume fraction (see Eq. 5) is all of the soot that entered the probe assembly. This soot was either collected on the filter or on the inner walls of the probe. Prior to the experiment, an aluminum dish along with two fresh PTFE filters were weighed. One of the filters was placed in the filter assembly shown in Fig. 1. The other filter was used to scrub the soot that was deposited on the inner walls of the probe using a plunger. The two filters and the aluminum dish were weighed again at the end of the experiment to determine how much soot entered the probe assembly. Typically 5 mg of soot was collected, of which 10% was accumulated in the probe assembly.

The mass concentration of the soot, M_s, was computed from the mass of soot collected on the filter, m_s, the ratio of the ambient temperature, T_∞, to the temperature at the probe entrance, T_p, and the total volume, V, of gas sampled based on the ambient temperature:

$$M_s = \frac{m_s}{V}\frac{T_\infty}{T_p}. \tag{1}$$

The estimated uncertainty (one standard deviation) in m_s, V, and T_p are 0.03 mg, 0.08 L, and 10 K, respectively. The radial profile for the temperature, T_p, and the mass concentration of soot, M_s, are shown in Fig. 2. It is seen that even with the use of the tripper plate, there is a radial dependence in the mass concentration, M_s, and temperature. In comparing the line of sight optical and single location gravimetric measurements, the radial average mass concentration was required. The radial average was computed as the arithmetic average of the three points shown in Fig. 2. The line of sight average mass concentration, M_s (ave) is equal to bM_s (center), where b (equal to 0.84) is the soot profile coefficient and M_s (center) is the mass concentration of soot at the center of the tube. Two factors affecting the uncertainty in the determination of b are lack of data at the wall of the chimney and excluding the curvature in the concentration profile. These effects result in an estimated uncertainty (one standard deviation) in b equal to ± 0.04.

The optical measurements were performed using a 15-mW 632.8-nm He–Ne laser and a solid-state photodiode with a 6-mm aperture, wedge beam splitter, and low-temperature coefficient feedback resistor. The path length, L, used for the optical measurements was equal to the inner diameter of the quartz tube (84 mm) with an estimated uncertainty of ± 2 mm. To prevent air entrainment into the chamber, "light" tubes were placed along optical line of sight (see Location B in Fig. 1). The plane of the glass windows was oriented 3° from perpendicular to the laser beam, to prevent interference from reflections. Nitrogen was purged through the tubes (at approximately 2 cm^3/s) to produce a constant path length (see Location C in Fig. 1).

Two different representations of Bouger's law are widely used for analyzing light transmission data. The first is used mainly for measurements of soot volume fraction in flames

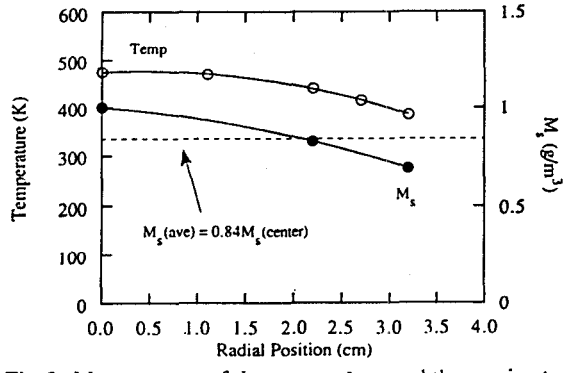

Fig. 2. Measurement of the temperature and the gravimetrically determined soot volume fraction at various radial positions.

and the second is used above the flame zone to estimate the soot yield from a fuel.

$$\frac{I}{I_0} = \exp\left(-\frac{K_a(1+\alpha_{sa})f_{va}L}{\lambda}\right) = \exp\left(-\frac{K_e f_{va} L}{\lambda}\right), \quad (2)$$

$$\frac{I}{I_0} = \exp(-\sigma_s M_s L), \quad (3)$$

where L is the path length, I is the transmitted laser intensity, I_0 is the incident laser intensity, f_{va} is soot volume fraction based on optical measurements, α_{sa} is the scattering to absorption ratio, and σ_s is the mass specific extinction coefficient. The nominal value of the ratio of transmitted to incident laser beam intensity, I/I_0 is 0.65 and the estimate uncertainty in $\ln(I/I_0)$ is 0.015. For soot particles of small optical dimension, the dimensionless absorption constant, K_a, is computed from the following formula obtained from Mie theory in the limit of small particle size [15]:

$$K_a = \frac{36\pi n_\lambda k_\lambda}{\left(n_\lambda^2 - k_\lambda^2 + 2\right)^2 + 4n_\lambda^2 k_\lambda^2} = 4.9, \quad (4)$$

using the dispersion relationship of Dalzell and Sarofim [15]. It is common practice in the combustion and fire community to set α_{sa} (scattering to absorption ratio) equal to zero to determine the soot volume fraction [4, 16]. However, the assumption that the scattering to absorption ratio α_{sa} is negligible is only valid for very small aggregates with optical sizes $2\pi R_g/\lambda$ less than 0.7 (where R_g is the radius of gyration of the agglomerate [17]). With this assumption, the Rayleigh-limit solution of the soot extinction constant can be used (Eq. 4). This practice may be valid when considering the primary particle diameter (which are typically 20–50 nm compared with source wavelength of 632.8 nm) as the dimension of interest. However, soot particles are aggregates composed of hundreds of primary particles and the average aggregate dimension can be of the same order of magnitude as the extinction source wavelength. Under this condition, the Rayleigh-limit assumption is no longer valid and using Eq. 4 to calculate the dimensionless extinction constant will result in large uncertainties. For example, the work of Köylü and Faeth [18], indicates that the scattering to absorption ratio for soot created in the overfire region of diffusion flames can be as high as 22%–41% (using $\lambda = 514.5$ nm).

HELIUM PYCNOMETRY DENSITY MEASUREMENTS

To determine the morphology and the structure of the soot generated in our experiments, soot particles were thermophoretically sampled. The soot samples were collected for durations of 3 and 10 s by inserting a carbon-coated 3-mm TEM grid into the postflame region at the location where gravimetric and optical measurements were performed. The soot was then examined with a TEM microscope at a nominal magnification of 2.3×10^4. Images were electronically digitized and the primary soot size was determined by an image analysis software for the electronic images. The average primary particle diameter measured for an equivalence ratio of 2.5 is about 22 nm, which is similar to the sizes measured in various flame [19]. Our objective was to determine the density of the individual primary spherules and not of the aggregate. Helium pycnometry is a technique that has been commonly used to measure the density of carbon black [20]. Helium is used because its small size can penetrate the voids between soot particles when they have been compacted.

The measurement of density requires the collection of a large sample on the order of 1 g or more. Approximately half of the flow exiting the tube was collected through a funnel to the cascade impactor operating at a flow of 28.3 L/min [12]. The soot was removed from the impactor stages, the water-cooled collection tube, funnel, and the top of the chimney. Approximately 1 h was required to collect 1 g soot when operating the burner at an equivalence ratio of 2.5.

The collected soot had a very low apparent density. The sample was compacted using a die to a density of about 0.04 g/cm^3. When the cell was half-filled with compacted soot, the actual volume occupied by the particles was

still only a couple of percent of the entire cell. After the cell was filled, it was outgassed at a temperature of 343 K and the density of the sample was determined. The measured density for the soot (1.7–1.8 g/cm^3) was slightly less than the value of 1.84 g/cm^3 obtained by Rossman and Smith for acetylene black [20]. Whereas the repeatability was within 1%, the accuracy may be somewhat lower because of the uncertainty associated with measurement of an extremely small volume. For the isokinetic calculations of the soot volume fraction, an average density of 1.74 g/cm^3 was used with an estimated uncertainty of ± 0.10 g/cm^3.

COMPARISONS OF GRAVIMETRIC AND OPTICAL MEASUREMENTS

The soot volume fraction based on gravimetric measurements, f_v, was obtained from the ratio of the mass concentration of soot, M_s, to the density of the soot, ρ_s.

$$f_v = \frac{M_s}{\rho_s}. \tag{5}$$

As discussed in the previous section, the density of the soot is taken to be the average of the helium pycnometry result of 1.74 g/cm^3. To compare with the optical measurements, which are based on a line of sight average, the radial average of the soot volume fraction, f_v(ave), equal to 0.84 f_v(center) was used [where f_v(center) is the volume fraction at the center of the tube].

For each experiment, extinction measurements were performed in conjunction with the gravimetric soot sampling experiments. Figure 3 displays the extinction measurements for acetylene/air flames with equivalence ratios of 2.3, 2.5, and 2.7. The data were averaged with a 0.1-s increment to reduce the fluctuations in the transmitted intensity. One minute of laser transmission was taken prior to flame ignition. The sharp reduction in the transmitted signal was due to the thick smoke produced by the initially very rich conditions at ignition. The sampling probe was inserted 1 min after ignition to avoid the initial transient soot accumulation. The signal transmitted through the soot

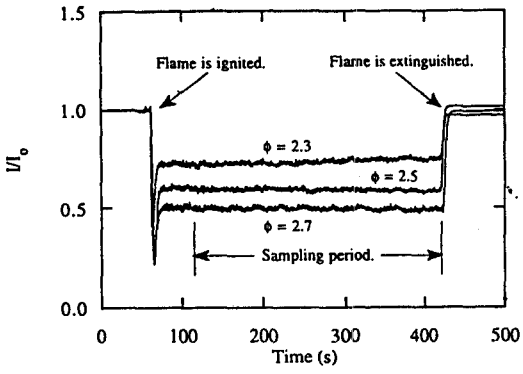

Fig. 3. Light extinction measurements as a function of time for rich acetylene/air premixed flames.

dispersion displays some fluctuations (caused by small changes in the path length); however, the average value remains nearly constant throughout the duration of the experiment. The flame was extinguished after 5 min (at t = 7 min) of soot sampling and the probe was immediately removed from the chimney.

Figure 4 displays the soot volume fraction as a function of equivalence ratios for both the gravimetric and optical measurements (f_{va} was calculated from Eq. 2 with $K_a = 4.9$, $\alpha_{sa} = 0$ for comparisons with gravimetric measurements). Table 1 displays f_v, f_{va}, and σ_s for the eight experiments. The optically determined soot volume fractions are approximately twice as large as the gravimetric measurements for all equivalence ratios. Another choice of re-

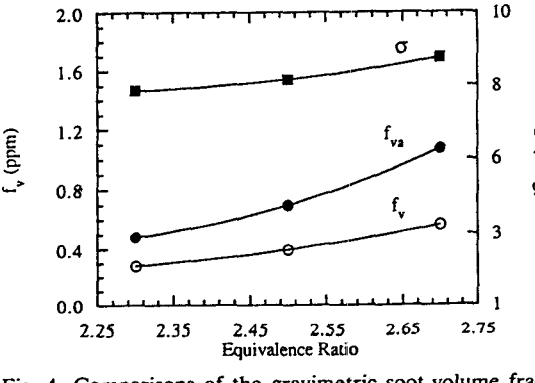

Fig. 4. Comparisons of the gravimetric soot volume fraction with optically-determined soot volume fraction (using Dalzell–Sarofim's dispersion relationship). Mass specific extinction coefficients is also plotted as a function of the equivalence ratio.

TABLE 1

f_v, f_{va}, α_s, and Corresponding K_e Values for Rich Acetylene/Air Premixed Flames[a]

Equivalence Ratio	f_v(ppm)	f_{va}(ppm)	σ_s(m^2/g)	K_e
2.3	0.28	0.48	7.6	8.4
2.5	0.41	0.78	8.7	9.3
2.5	0.41	0.68	7.6	8.2
2.5	0.41	0.72	8.0	8.7
2.5	0.41	0.71	7.9	8.5
2.5	0.33	0.57	7.9	8.5
2.5	0.31	0.51	7.4	8.0
2.7	0.56	1.34	8.6	9.3
	Average Values		8.0	8.6

[a] Gravimetric soot volume fraction f_v, optical soot volume fraction f_{va}, specific extinction coefficient σ_s, and calculated dimensionless extinction coefficient K_e for equivalence ratios of 2.3, 2.5, and 2.7.

fractive index could lead to better or poorer agreement between the optical and gravimetric measurements. For example, the calculated absorption constant using the various indices of refraction can vary by a factor of 2 [11]. In addition to the uncertainty in the optical properties, replacing K_e with K_a neglects light scattering. This can result in as much as 25% underestimate of K_e and 33% overestimate of the soot volume fraction. However, the gravimetrically determined soot volume fraction is more accurate. Furthermore, by setting f_{va} equal to f_v (since measurements were performed at the same location), one can compute the value of K_e consistent with the accurately determined soot volume fraction using the following relationships:

$$f_{va} = \frac{-\ln\left(\frac{I}{I_0}\right)\lambda}{K_e L} = f_v, \tag{6}$$

$$K_e = \frac{-\ln\left(\frac{I}{I_0}\right)\lambda}{f_v L}. \tag{7}$$

Table 1 also lists the K_e calculated from each experiment. The average value and 2 standard deviations of K_e is 8.6 ± 1.5 (see Section on uncertainty analysis).

Using the dimensionless extinction constant of 8.6 instead of 4.9, the optically determined soot volume fractions are calculated and compared with the gravimetric measurements in Fig. 5. This figure demonstrates that a single value of K_e can be used to correct the light extinction data for soot generated under different operating conditions.

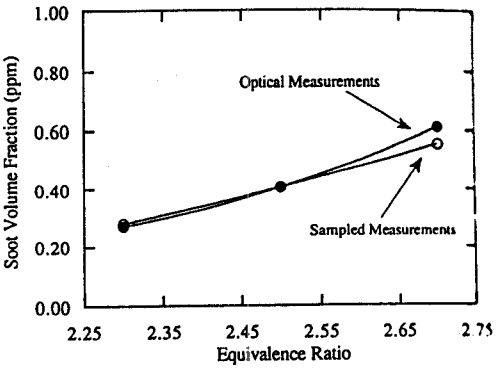

Fig. 5. Comparison of the gravimetric soot volume fraction with optically determined soot volume fraction (using K_e = 8.6).

Also in Fig. 4 we demonstrate that the average mass specific extinction constant, σ_s, is relatively insensitive to the equivalence ratio. The only difference between specific extinction constant, σ_s, and the dimensionless extinction constant, K_e, is the product of the density of soot and the laser wavelength [$K_e/\sigma_s = \rho_s\lambda$]. The mean value of all the measurements for σ_s is 8.0 ± 1.5. This is in good agreement with typical values of σ_s measured for soot produced from different fuels including wood, crude oil, heptane and polyurethane as shown in Table 2.

TABLE 2

Mass Specific Extinction Coefficients for Soot Created from Various Fuels[a]

σ (m^2/s)	Fuel	Reference
8.0 ± 0.5	Acetylene	Present study
7.8 ± 1.2	Crude oil	Dobbins et al. (1993)
8	Hydrocarbon fuels and plastic	Patterson et al. (1991)
7–8	Heptane	Mulholland et al. (1989)
9	Wood	Mulholland et al. (1989)
8.5–9.1	Polyurethane	Mulholland et al. (1989)
10–12	Liquified petroleum gas, mainly butane	Colbeck et al. (1989)

[a] Specific extinction coefficients measured for various fuels.

DISCUSSION

Newman and Steciak [7] determined the soot particle density from the observed linear relationship between soot volume fraction and particle mass concentration for overventilated diffusion flames. The soot volume fraction was determined using an extinction constant calculated from multi-wavelength transmission analysis based on Mie theory (refractive indices of Lee and Tien were employed [21]). There is a large discrepancy between our measured soot density of 1.74 g/cm^3 and their calculated density of 1.1 g/cm^3. The density of 1.1 g/cm^3 is also significantly lower than the values reported by other investigators for carbonaceous particulates. For example, Rossman and Smith measured a density of 1.84 g/cm^3 for acetylene black [20]. The low value obtained by Newman and Steciak can be attributed to our observation that the optical measurements overestimate the soot volume fraction [11].

By measuring the dimensionless extinction constant, K_e, we avoid issues related to the refractive index, fractal structure of soot and multiple scattering within the agglomerate in calculating the extinction constant. As discussed above, the ratio K_e/σ_s is equal to product of the density times the laser wavelength. The densities reported for carbonaceous particulates vary from approximately 1.70 to 2.00 g/cm^3. The independence of the mass specific extinction constant as a function of fuel type (Table 2) suggests that the measured value of K_e equal to 8.6 ± 1.5 is a useful estimate for soot generated from a wide range of fuels at $\lambda = 632$ nm.

In previous work by Dobbins and coworkers, the specific extinction constant was found to vary nearly inversely with the wavelength from 450 to 1000 nm [26]. The dimensionless extinction constant, K_e, which is proportional to the product of σ_s and wavelength, λ is thus approximately constant. Newman and Steciak also report that the dimensionless extinction constant is relatively insensitive to the laser wavelength [7].

In this study as well as several others referred to above [7, 12, 26], the soot volume fraction measurements are made in the postflame zone. Köylü and Faeth [18] determined that the scattering to absorption ratios for large soot aggregates created in the overfire region of acetylene, ethylene and propane diffusion flame are 41%, 29%, and 22%, respectively at $\lambda = 514.5$ nm. (The corresponding scattering to extinction ratios are 29%, 22%, and 18%.) These scattering to extinction ratios are expected to decrease for experiments in which longer wavelength lasers are used (i.e., $\lambda =$ 632.8 nm as in the present study). Thus, even for these cases in which scattering is expected to be significant, the estimated total contribution of the scattering to the extinction coefficient at a source wavelength of 632 nm is 23%. There is also great interest in the soot volume fraction measured within laminar and turbulent flames. The approach that has been widely used is to perform light extinction measurements and then use Eq. 2 with α_{sa} set equal to zero. As discussed above, this leads to an overestimate by a factor of 1.75 (ratio of 8.6/4.9) in the post-flame region. While the soot agglomerates will be smaller in some regions of the flame compared to the post-flame, they are still large enough that scattering will contribute to the light extinction [17, 25]. For these reasons, the use of $K_e = 8.6$ measured in the present study is expected to provide a more accurate measurement of soot within the flame and in the postflame region.

Still, more work is needed to better define the degree of scattering in the flame zone. Within the flame, there are also issues to be resolved regarding the refractive index. For example, Habib and Vervisch [22] found differences in the refractive index of soot generated from different fuels (including methane, propane and ethylene). Chang and Charalampopoulos [23] performed experiments using a premixed flame and found variations of the refractive index as a function of height above the burner suggesting effects of temperature and the soot C/H ratio. For these reasons, future experiments are planned to investigate the effects of using different fuels, different configurations (diffusion flame and premixed flame), various sampling temperatures and extinction wavelengths on the dimensionless extinction constant of soot.

An important application of the simultaneous optical/gravimetric measurements de-

scribed in this study is for determining the dimensionless extinction constant for flame-generated particles containing both soot and inorganic materials such as silica for which optical properties (such as the refractive index) are not available. Silicon containing fuels such as hexamethyldisiloxane produce significant amounts of carbonaceous/silica particles, however, concentration measurements cannot be made by light extinction without accurate extinction constants [27].

UNCERTAINTY ANALYSIS

An uncertainty analysis for K_e was performed to define the 95% confidence interval which is both a NIST policy and a widely adopted international practice for reporting uncertainty estimates [28]. The combined standard uncertainty of the result y is estimated by the *law of propagation of uncertainty* as the positive square root of the estimated variance, $u_c^2(y)$, obtained from

$$u_c^2(y) = \sum_{i=1}^{N} \left[\frac{\partial f}{\partial x_i} \right]^2 u^2(x_i), \tag{8}$$

where $u(x_i)$ is the estimated standard deviation of the variables x_i. The uncertainty analysis is performed for six quantities, M_s, $M_{s,ave}$, f_{va}, f_v, σ_s, K_e. In Table 3, the nominal value and the estimated standard deviation for each x_i are given in addition to the expanded uncertainty, U.

We report the results in Table 3 as an expanded uncertainty, $U = 2u_c$, to define an interval having a level of confidence of approximately 95%. The expanded uncertainty for K_e is approximately ± 1.5. All measured values given in Table 1 are in a narrower range of 8.0 to 9.3.

The largest uncertainties are in the density of the soot with $\sigma_{ps}/\rho_s = 0.06$ and the soot profile coefficient, $\sigma_b/b = 0.05$. Significant reduction of the uncertainty in ρ_s is possible by collecting more sample and using increased compaction so that the effective sample volume is increased in the pycnometer. Reductions in the uncertainty of b can be accomplished by establishing a more uniform environment by heating the walls.

CONCLUSIONS

By combining gravimetric measurements of the collected soot with soot density measurements using helium pycnometry, an accurate value of the soot volume fraction was obtained for rich

TABLE 3

Nominal Values and the Associated Individual Uncertainties in the Measured Parameters that Contribute to the Expanded Uncertainty in K_e

Physical Quantity	Nominal Value	Contributing Variable	Nominal Value	$\sigma(x_i)/x_i$	U, Expanded Uncertainty[a]	U/y[b]
M_s	0.78 g/m^3	m_s	5.00 mg	0.006	0.05 g/m^3	0.06
		V	4.00 L	0.020		
		T_p	475 K	0.021		
M_{ave}	0.66 g/m^3	M_s	0.78 g/m^3	0.030	0.07 g/m^3	0.11
		b[c]	0.84	0.050		
f_{va}	0.69 ppm	$\ln(I/I_0)$	−0.43	0.035	0.07 ppm	0.08
		L	0.084 m	0.024		
f_v	0.38 ppm	M_{ave}	0.66 g/m^3	0.055	0.06 ppm	0.16
		ρ_s	1.74 g/cm^3	0.057		
σ_s	7.8 m^2/g	$\ln(I/I_0)/L$[d]	−5.12/m	0.040	1.1 m^2/g	0.14
		m_{ave}	0.38×10^{-6} g/m^3	0.055		
K_e	8.5	$\ln(I/I_0)/L$	−5.12/m	0.040	1.5	0.18
		f_v	0.38 ppm	0.08		

[a] Corresponds to two standard deviations.
[b] Corresponds to nominal value of the variables in column 2.
[c] Corresponds to the soot profile coefficient, M_s(ave) = bM_s(center).
[d] Same relative uncertainty as f_{va}.

acetylene premixed flames. The temperature and soot concentration profiles were measured to compare the line of sight light extinction measurement with the point sampling gravimetric measurements. By calibrating the optical measurements with the gravimetric soot volume fractions, a dimensionless extinction constant, K_e, of 8.6 $\pm$ 1.5 was measured. It was also found that the mass specific light extinction coefficient was equal to 8.0 $\pm$ 1.1 m^2/g, which is consistent with measurements reported in the literature for a soot produced from a variety of fuels [8, 20, 24, 29]. The K_e measured in this study is recommended as a useful first-order estimate for computing soot volume fraction based on light extinction measurements for soot generated from a variety of fuels for both small and large scale flames.

The authors gratefully acknowledge helpful discussions and advice provided by Dr. Christopher Shaddix and Mr. Nelson Bryner of NIST. We also acknowledge Mr. Eric Steel and Ms. Lin Lum of NIST for the microscopy and the pycnometry experiments.

REFERENCES

1. Santoro, R. J., Yeh, T. T., Horvath, J. J. and Semerjian, H. G., *Combust. Sci. Technol.* 53:89 (1987).
2. Harris, S. M. and Weiner, A. M., *Combust. Sci. Technol.* 31:156 (1983).
3. Choi, M. Y., Hamins, A., Rushneier, H. and Kashiwagi, T., *Twenty-Fifth Symposium (International) on Combustion*, in press.
4. Klassen, M., Ph.D. thesis, University of Maryland, Department of Mechanical Engineering, 1992.
5. Blinov, V. I. and Khudiakov, G. N., *Dokl. Akad. Nauk.* USSR, 113:241 (1957).
6. Burgess, D., and Hertzberg, M., in *Heat Transfer in Flames* (N. H. Afgan and J. M. Beer, Eds.), Hemisphere Press, New York, 1974, p. 413.
7. Newman, J. S., and Steciak, J., *Combust. Flame* 67:55 (1987).
8. Mulholland, G. W., Henzel, V., and Babrauskas, V., in *Proceedings of the Second International Symposium on Fire Safety Science* (T. Wakamatsu, Y. Hasemi, A. Sekizawa, P. G. Seeger, P. J. Pagni, and C. E. Grant, Eds.) Hemisphere, New York, 1989, p. 347.
9. Mulholland, G. W., *Soot Production and Properties*, SFPE Handbook of Fire Protection Engineering (P. J. DiNenno, Ed.), 1988, p. 368.
10. Benner, B. A., Bryner, N. P., Wise, S. A., and Mulholland, G. W., *Environ. Sci. Technol.* 24:1418 (1990).
11. Choi, M. Y., Hamins, A., Mulholland, G. W. and Kashiwagi, T., *Combust. Flame*, in press.
12. Choi, M. Y., Mulholland, G. W., Hamins, A. and Kashiwagi, T., Eastern States Section of the Combustion Institute, Princeton, NJ, October 25–28 (1993).
13. Leonard, S., Mulholland, G. W., Puri, R., and Santoro, R. J., *Combust. Flame*, submitted.
14. Liu, B. Y. H., Pui, D. Y. H. and Bubow, K. L., *Characteristics of Air Sampling Filter Media*, Aerosols in the Mining and Industrial Work Environments, (V. A. Marple and B. Y. H. Liu, Eds.), Ann Arbor Science, 1983, Vol. 3, Chap. 70, p. 989.
15. Dalzell, W. H., and Sarofim, A. L., *J. Heat Transfer* 91:100 (1969).
16. Sivathanu, Y. R., and Faeth, G. M., *Combust. Flame* 81:150 (1990).
17. Mountain, R. D., and Mulholland, G. W., *Langmuir* 4:1321 (1988).
18. Köylü, U. O., and Faeth, G. M., *J. Heat Transf.* p. 152 (1994).
19. Megaridis, C. M., Personal communications, 1994.
20. Rossman, R. P., and Smith, W. R., *Ind. Eng. Chem.* 35:972 (1943).
21. Lee, S. C., and Tien, C. L., *Eighteenth Symposium (International) on Combustion*, The Combustion Institute, Pittsburgh, 1981, p. 1159.
22. Habib, Z. G., and Vervisch, P., *Combust. Sci. Technol.* 59:261 (1988)
23. Chang, H., and Charalampopoulos, T. T., *Proc. R. Soc. Lond. A.* 430:577 (1990).
24. Patterson, E. M., Duckworth, R. M., Wyman, C. M., Powell, E. A., and Gooch, J. W., *Atmos. Environ.* 25A:2539 (1991).
25. Vander Wal, R. V., Choi, M. Y., and Lee, K. O., submitted.
26. Dobbins, R. A., Mulholland, G. W., and Bryner, N. P., *Atmos. Environ.* 28:889 (1994).
27. Buch, R., Private communication, 1993.
28. Taylor, B. N., and Kuyatt, C. E., NIST Technical Note 1297 (1993).
29. Colbeck, I., Hardman, E. J., and Harrison, R. M., *J. Aerosol Sci.* 20:765 (1989).

Received 24 May 1994; revised 14 December 1994